ELSEVIER

Thermochimica Acta 296 (1997) 23–29

thermochimica acta

Thermal analysis of Ag–As–Se chalcogenide glasses

N. Zotov[1*], C. Wagner, F. Bellido, L.M. Rodriguez, R. Jimenez-Garay

Departamento de Fisica de la Materia Condensada, Universidad de Cadiz, 11510 Puerto Real, Spain

Received 12 December 1996; received in revised form 26 February 1997; accepted 3 March 1997

Abstract

Differential scanning calorimetry measurements for silver-containing chalcogenide glasses along the pseudo-binary tie line $(Ag_2Se)_x(AsSe)_{(1-x)}$ with high silver content are reported and discussed. The glass-transition temperatures (T_g) are independent of the Ag content. No correlation between T_g and the first-nearest neighbour mean coordination numbers is observed for $x > 0.25$, which indicates that the onset of viscous flow is independent of the rigidity of the glassy network in these chalcogenide glasses. The crystallization proceeds in three stages. X-ray diffraction phase analysis has shown that the hexagonal (metastable) modification of the $AgAsSe_2$ phase is formed in the first crystallization process; it is then transformed into the tetragonal $AgAsSe_2$ phase, followed by crystallization of the Ag_3AsSe_3 phase. The enthalpy of primary crystallization decreases with increasing Ag content, accompanied by an increase of the activation energy of primary crystallization and the thermal stability of the supercooled liquid, which suggests a change of the crystallization mechanism. © 1997 Elsevier Science B.V.

Keywords: Chalcogenide glasses; Glass-transition temperatures; Kinetics of crystallization

1. Introduction

Silver-containing chalcogenide glasses have received a great amount of consideration [1], which was largely stimulated by the fact that their electric conductivity changes from predominantly electronic, at low Ag contents, to predominantly ionic at high silver contents [1,2]. However, the interrelation between their local structure and transport as well as thermal properties is still poorly understood, although there are a lot of structural studies, especially on Ag–As–Se glasses, including X-ray diffraction [3,4], neutron diffraction [5,6], Extended X-ray absorption fine-structure (EXAFS) spectroscopy [7] and reverse Monte-Carlo (RMC) simulations [8].

Several authors have related the increase of the mean coordination number in chalcogenide glasses to an increase of the glass-transition temperature (T_g) (Ref. [9,10] and references therein). However, the thermal data for the Ag–As–Se glasses are very scarce [1,11]. The present work was undertaken to systematically determine the compositional dependence of the glass-transition temperature and activation energy for viscous flow, the thermal stability, the enthalpies of crystallization and the crystallization kinetics of bulk quenched $(Ag_2Se)_x(AsSe)_{(1-x)}$ glasses with high sil-

*Corresponding author. Tel.: 49-921-553739; fax: 49-921-553769; e-mail: nikolay.zotov@uni-bayreuth.de.

[1]On leave from the Central Laboratory of Mineralogy and Crystallography, Bulgarian Academy of Sciences, Sofia 1000, Bulgaria

PII S0040-6031(97)00112-3

ver content. We were specially interested in Ag–As–Se glasses with high silver content,in which case their electric conductivity is predominantly ionic due to the high mobility of the Ag^+ ions.

Ternary homogeneous Ag–As–Se glasses are formed in 2 overlapping regions along the As_2Se_5–Ag_2Se and the AsSe–Ag_2Se pseudo-tie lines of the ternary phase diagram [11]. However, the form of the glass-formation region in the compositional triangle allows amorphous alloys of high silver content to be obtained only along the AsSe–Ag_2Se tie line. That is why, three $(Ag_2Se)_x(AsSe)_{(1-x)}$ glasses with nominal composition $x = 0.25$, 0.40 and 0.55, covering the high-Ag part ($0.25 \leq x \leq 0.60$) of the glass-formation region, were synthesized for the present study.

2. Experimental

2.1. Sample preparation

Three $(Ag_2Se)_x(AsSe)_{(1-x)}$ chalcogenide glasses with nominal composition $x = 0.25$, 0.40 and 0.55 were prepared by melt quenching. First, pure silver (99.99%, Aldrich), arsenic (99.9999%, Aldrich) and selenium (99.999%, Aldrich) were ground in agate mortar, sewed through a mesh to obtain grain size of less than 64 μm and mixed together to obtain ~8 g of the corresponding composition. For each sample, the powder mixture was put into quartz tube of 6 mm i.d. and repeatedly evacuated–refilled with He. The tube was then sealed with oxyacetylene burner while the residual gas pressure was $\sim 1 \times 10^{-2}$ Pa. The as-prepared ampoules were kept at 800°C for four days in a horizontal furnace and then quenched in ice water. In order to obtain good homogeneity of the samples, the ampoules were rotating with at about 6 rpm. The composition of the final glassy alloys was determined using a Jeol JSM 820 SEM with EDAX X-ray dispersive analyser. The actual compositions ($x = 0.27$, 0.39 and 0.54) are close to the nominal and the samples will be denoted hereafter as AG27, AG39 and AG54, respectively.

2.2. Thermal analysis

All differential scanning calorimetry (DSC) measurements were carried out on a Perkin–Elmer D7 thermal analyser. The thermal analyser was carefully calibrated from 50° to 450°C against the known temperatures and enthalpies of melting for In and Zn. During all runs, the sample chamber was purged with dry N_2. The samples consisted of ~20 mg powder in crimped (but not hermetically sealed) Al pans. All measurements were referenced to an empty Al pan. Special care was taken for reproducibility of the base line by always using the same orientation of the Pt lids. The DSC curves were measured at heating rates of $\beta = 2, 4, 10, 20$ and 40 K min^{-1}. The crystallization temperatures (T_p) were determined as the temperatures of maximum crystallization rate. The glass-transition temperatures (T_g) were determined as the extrapolated onset temperatures of the glass transition [12] (see Fig. 1). Repeated measurements on several samples with the same heating rate indicate

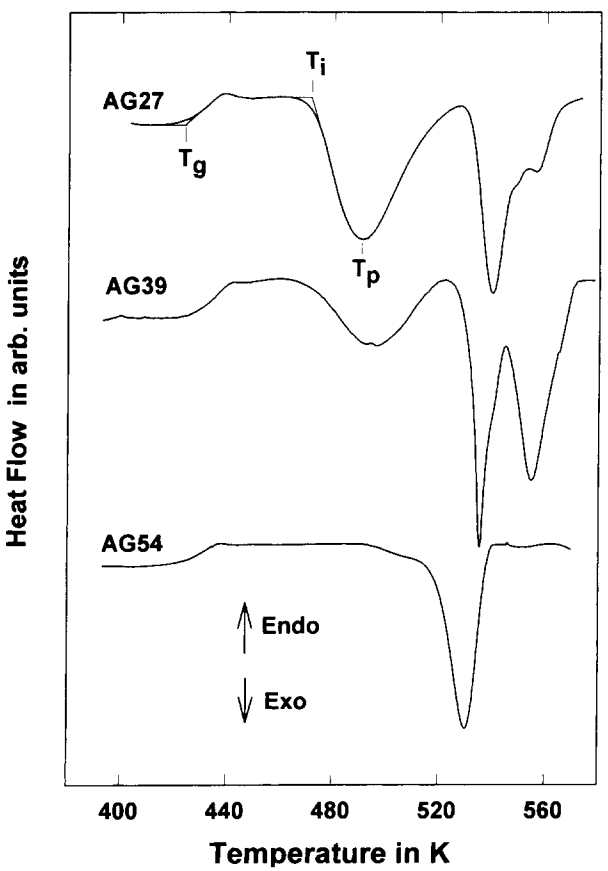

Fig. 1. Differential scanning calorimeter curves of Ag–As–Se glasses (heating rate at 10 K min^{-1}).

that the experimental accuracy of T_g and T_p is $\sim\pm 2$ K and the accuracy in the enthalpies of crystallization ± 3 J/g.

2.3. X-ray diffraction analysis

X-ray diffraction phase analysis of the crystallization products was carried out on a Philips PW1830 automatic powder diffractometer equipped with automatic divergence slit, diffracted beam graphite monochromator and proportional detector. All measurements were made with step $\Delta 2\Theta = 0.02°$ and a time of 5 s per step, using CuK_α radiation.

3. Results

3.1. Glass transitions

Typical DSC curves for all three samples are shown in Fig. 1. The melting endotherms for the AG27, AG39 and AG54 samples are at ~620, 623 and 647 K, respectively. They are well-separated from the crystallization exotherms and will not be discussed further.

Only one glass transition is observed for all samples, indicating that they represent *homogeneous* glasses. The T_g value for the AG27 sample, 429 ± 1 K, measured at a heating rate $\beta = 10$ K min^{-1}, compares very well with the value 430 K, reported by Benmore and Salmon [6] for the $(Ag_2Se)_{0.25}(AsSe)_{0.75}$ composition using the same heating rate. The T_g values of Houphouet-Boigny et al. [11], determined at a heating rate $\beta = 4$ K min^{-1} are, however, slightly higher than the values measured by us at a heating rate $\beta = 5$ K min^{-1} for similar compositions.

From the heating-rate dependence of the glass-transition temperature, one can determine the glass-transition temperature, T_g^0, not affected by kinetic factors, regarded as the temperature of an underlying thermodynamic glass–liquid transition at $\beta \rightarrow 0$ [13]. The T_g values were fitted by the equation, $T_g = T_g^0 + \beta_g \ln(\beta)$, proposed by Lasocka [14] (Fig. 2). The activation energies (E_g) of the glass transition were determined using the equation, $\ln(\beta) = -E_g/RT_g + \text{const}$ (where R is the gas constant), proposed by Moynihan et al. [15] (see Fig. 3). The thermal stability of the supercooled liquid ΔT_L, at

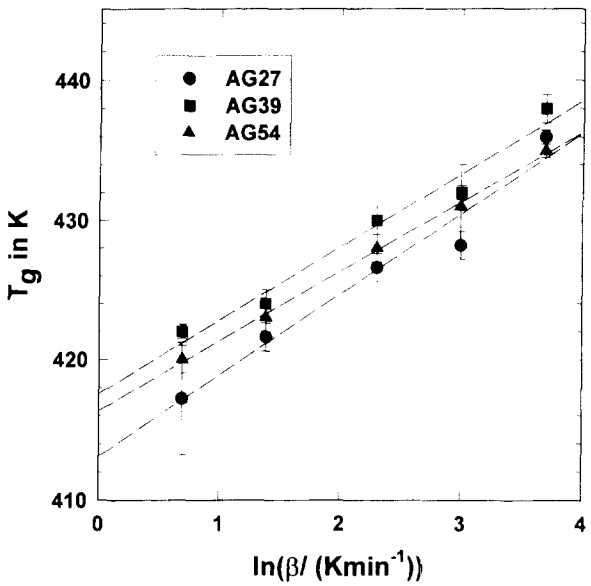

Fig. 2. Plot of T_g vs. ln(β) (β in K min^{-1}): (●) – AG27 sample; (■) – AG39 sample; and (▲) – AG54 sample. The dashed lines are linear fits through the data points.

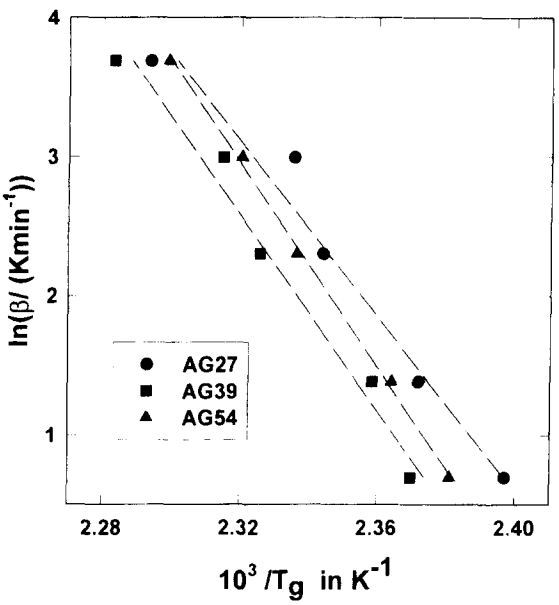

Fig. 3. Plot of ln(β) vs. $1/T_g$ (β in K min^{-1}, T_g in K): (●) – AG27 sample; (■) – AG39 sample; and (▲) – AG54 sample. The dashed lines are linear fits through the data points.

Table 1
Glass-transition results for the investigated Ag–As–Se glasses

Sample	T_g^0/K	β_g	E_g/(kJ/mol)	$\Delta C_p(T_g)$/(J/gK)	ΔT_L/K
AG27	413±5	5.8±1.9	265±30	0.29±0.01	46±4
AG39	418±5	5.3±1.9	237±25	0.44±0.05	44±12
AG54	416±4	5.0±1.9	228±10	0.59±0.17	89±11

Table 2
Enthalpies of crystallization (in J/g) of the Ag–As–Se glasses

	Crystallization stage			
Sample	1	2	3	Total enthalpy
AG27	26.0±0.5	12.0±2.5	7.0±1.0	45.0±3.0
AG39	12.0±1.0	14.0±2.0	21.0±1.5	47.0±3.0
AG54	4.0±0.5	23.0±0.2		27.0±0.5

* The standard deviations are calculated from the least-squares decomposition.

a given heating rate, was estimated as $\Delta T_L = T_i - T_g$, where T_i is the onset temperature of the first crystallization peak (see Fig. 1). In the first approximation, ΔT_L is independent of the heating rate since both T_i and T_g increase with increasing β. That is why the ΔT_L values for each composition were averaged over all heating rates. The change of the heat capacity at constant pressure between the glass and the supercooled liquid at T_g, $\Delta C_p(T_g)$, was calculated from a plot of $\Delta C_p(T_g)$ vs. $\ln(\beta)$.

The results obtained together with the corresponding standard deviations calculated from the linear regression fits are given in Table 1. The glass-transition temperature T_g^0 and the rate constant β_g are within error limits independent of the composition. It is not clear whether the decrease of E_g is a real effect or it is also independent of composition. The increase of the heat capacity $\Delta C_p(T_g)$ with increasing Ag content means that the excess configurational entropy of the supercooled liquid above T_g increases with increasing Ag content and contributes to the increased stability of the supercooled liquid.

3.2. Enthalpies of crystallization

The AG27 and AG39 samples exhibit three crystallization peaks, while in the AG54 sample only two peaks are observed (Fig. 1). Gaussian decomposition of the DSC curves for the AG27 and AG39 samples revealed an additional weak peak at $\sim 540 \pm 8$ K, which will not be considered separately in the subsequent analysis. Several crystallization peaks were also reported for some of the $(Ag_2Se)_x(AsSe)_{(1-x)}$ glasses, prepared by Houphouet-Boigny et al. [11]. In general, multiple crystallization peaks are characteristic for other ternary chalcogenide glasses in the Cu–As–Se and Cu–As–Te systems [16–18] as well.

In order to determine all enthalpies of crystallization, we have used a least-squares profile decomposition with Gaussian functions of the DSC curves measured at a heating rate 10 K min^{-1} (at which the thermal analyser was calibrated). The goodness-of-fit factors obtained are between 2.7 and 9.9% for all samples. The enthalpies of crystallization are given in Table 2. The enthalpy of the first crystallization process (ΔH_1) decreases almost linearly with increasing Ag_2Se content. The extrapolated x value at which ΔH_1 becomes zero, $x = 0.57 \pm 0.17$ compares very well with the position of the amorphous–crystalline boundary at $x = 0.6 \pm 0.1$, determined by Houphouet-Boigny et al. [11].

3.3. Kinetics of primary crystallization

Different mathematical methods have been proposed in the literature for the analysis of data obtained from non-isothermal measurements (see, for review, Ref. [19] and references therein). Comparative studies of the activation energies of As–Se–Te chalcogenide glasses [20], determined by different non-isothermal

methods, have shown that most of these methods give (within error limits) similar results. That is why, only the method proposed by Gao and Wang [21], commonly applied for the analysis of DSC data of glasses was used in the present study. According to this method, a plot of $\ln((d\alpha/dt)|_p)$ vs. $1/T_p$ yields a straight line with a slope E_a/R (where E_a is the activation energy) and intercept, proportional to the frequency factor K_0. The reaction order, n, in this approach is given by the equation, $n = (d\alpha/dt)|_p/0.37K_p$. In these expressions $\alpha(t)$ is the volume fraction of the crystallized phase, $(d\alpha/dt)|_p$ the maximum crystallization rate at T_p and $K_p = \beta E_a/RT_p^2$. K_p, $(d\alpha/dt)|_p$ and n were calculated for all heating rates and the values averaged.

The overlap between the two crystallization peaks, observed in the AG54 sample, is significant. In order to determine the kinetic parameters in this case, profile decomposition for all heating rates was performed. The plots of $\ln(d\alpha/dt|_p)$ vs. $1/T_p$ are shown in Fig. 4. The activation energies and the frequency factors of primary crystallization, as well as the corresponding regression coefficients are given in Table 3. The standard deviation of E_a for the AG54 sample is larger because the first crystallization peak in this case is very weak and overlaps strongly with the second peak. The reaction order of primary crystallization is, within error limits, the same for all samples and equals 1.1 ± 0.2. Similar values for n have been obtained for other As–Se chalcogenide glasses [22].

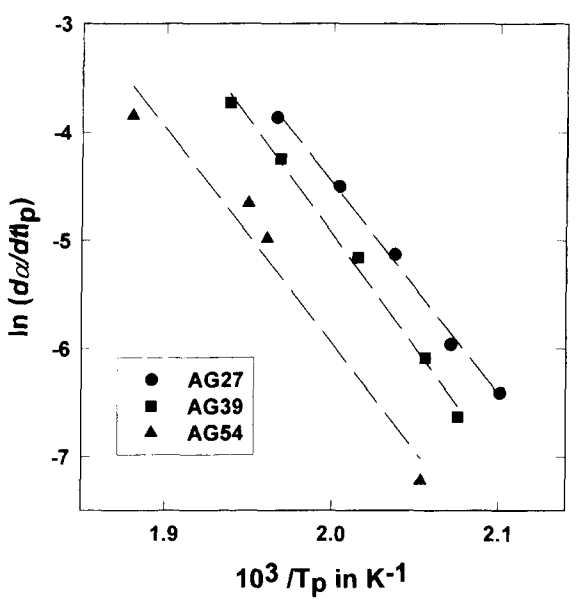

Fig. 4. Plots of $\ln(d\alpha/dt|_p)$ vs. $1/T_p$ (T_p in K): (●) – AG27 sample; (■) - AG39 sample; and (▲) - AG54 sample. The dashed lines are linear fits through the data points.

Table 3
Frequency factors (K_0) and activation energies of primary crystallization (E_a) of the investigated Ag–AsSe glasses

Sample	K_0/s^{-1}	E_a/(kJ/mol)	r^*
AG27	2.1×10^{15}	162±7	0.9975
AG39	2.5×10^{16}	174±8	0.9974
AG54	1.0×10^{8}	211±64	0.9419

* Regression coefficient.

4. Discussion

The glass-transition temperatures obtained in the present study, as well as the results of Houphouet-Boigny et al. [11], indicate that for $x > 0.2$ the T_g values of the $(Ag_2Se)_x(AsSe)_{(1-x)}$ chalcogenide glasses are practically independent of the Ag_2Se content.

Several empirical expressions [23–26] have been proposed, relating the glass-transition temperature to the mean coordination number ⟨CN⟩. However, our recent X-ray diffraction radial distribution functions analysis of the investigated Ag–As–Se glasses [8], as well as the EXAFS results for other Ag–As–Se compositions [7] along the same tie line, show that there is a strong increase of ⟨CN⟩ with increasing Ag content from 2.4 for the AG27 sample to 3.6 for the AG54 sample. Evidently, the relationship between the onset of viscous flow and the rigidity of the glassy network, traditionally associated with the mean coordination number [27,28], is more complex for the investigated Ag–As–Se glasses.

In order to understand further the kinetics of crystallization of the investigated glasses along the AgSe–Ag_2Se tie line, we have heated in the DSC apparatus ($\beta = 10$ K min^{-1}) samples to temperatures above the corresponding crystallization peaks, which were then rapidly quenched. The samples obtained were analysed by X-ray diffraction.

The crystallization in all three glasses begins with the formation of the hexagonal modification of the

$AgAsSe_2$ phase [29]. The refined lattice parameters of the h-$AgAsSe_2$ phase for the AG27 and AG39 samples are similar ($a = 3.92 \pm 0.01$ Å, $c = 20.38 \pm 0.01$ Å) and very close to the data of Voroshilov et al. [29]. With increasing Ag content, the amount of the h-$AgAsSe_2$ phase in the X-ray diffraction patterns decreases. This explains well the observed decrease of the enthalpy (Table 2) of primary crystallization, which is directly proportional to the total amount of crystallized phase. Evidently, the increase of the Ag_2Se content leads to reduction of the nucleation and growth rates of the $AgAsSe_2$ phase, resulting in higher activation energies (Table 3).

The amount of the remaining non-crystallized amorphous phase after the first crystallization step is practically zero for the AG27 sample and increases with increasing Ag content. The second crystallization process ($T_p = 537 \pm 2$ K), well-separated in the AG39 and AG27 samples, represents a transition from the h-$AgAsSe_2$ phase to the so-called tetragonal (t) $AgAsSe_2$ phase [29]. Unfortunately, the structure of the t-$AgAsSe_2$ phase is not known and will be subject of future studies.

The last crystallization process involves the formation of the low-temperature Ag_3AsSe_3 phase [30] from the remaining non-crystallized supercooled liquid. In the AG54 samples, quenched after the last crystallization peak, we do not observe h-$AgAsSe_2$ phase but only the t-$AgAsSe_2$ phase, which indicates that the processes of the h $\rightarrow$ t-$AgAsSe_2$ transformation and the crystallization of the Ag_3AsSe_3 phase overlap for $x \geq 0.5$.

The amount of the Ag_3AsSe_3 phase is practically zero in the AG27 sample, quenched after the last crystallization peak, and increases with increasing Ag_2Se content for the AG39 and AG54 samples at the expense of the t-$AgAsSe_2$ phase, in accordance with the Ag–As–Se phase diagram [31,32]; namely, the investigated $(Ag_2Se)_x(AsSe)_{(1-x)}$ glasses lay in the triangle As–$AgAsSe_2$–Ag_3AsSe_3 of the ternary phase diagram and the amount of Ag_3AsSe_3 phase, according to the lever rule, increases with decreasing the distance to the ternary point Ag_3AsSe_3, in other words with increasing x. It should be pointed out, however, that the binary join $AgAsSe_2$–Ag_3AsSe_3 lies outside the glass-formation region [11]. The refined lattice parameters of the Ag_3AsSe_3 phase for the AG39 sample ($a = 11.327 \pm 0.004$ Å, $c = 8.789 \pm 0.005$ Å) and for the AG54 sample ($a = 11.29 \pm 0.01$ Å, $c = 8.75 \pm 0.01$ Å) are in very good agreement with the lattice parameters reported in [29,30] and indicate that no solid solutions are formed.

5. Conclusions

The glass-transition temperatures, enthalpies of crystallization and kinetics of crystallization of three $(Ag_2Se)_x(AsSe)_{(1-x)}$ chalcogenide glasses with high silver content ($x = 0.27$, 0.39 and 0.54) have been determined by differential scanning calorimetry.

The experimentally determined glass-transition temperatures are, within error limits, compositionally invariant. Evidently, for overconstrained glasses (mean coordination number > 2.4 [27]) the rigidity of the glassy network does not play any more the main role for the onset of viscous flow.

The investigated Ag–As–Se glasses crystallize in three steps, the second and third of which merge into one DSC peak for $x \geq 0.5$. The crystallization begins with the formation of the hexagonal modification of the $AgAsSe_2$ phase, followed by crystallization of the remaining supercooled liquid into the Ag_3AsSe_3 phase. The refined lattice constants of the $AgAsSe_2$ and Ag_3AsSe_3 phases are in very good agreement with the literature data, which not only confirms the phase identification but indicates that no solid solutions are formed. The compositional dependence of the enthalpy of primary crystallization confirmed the position of the amorphous–crystalline boundary at about $x = 0.6$ along the AsSe–Ag_2Se tie line which has been already approximately determined by X-ray diffraction [11].

The slight increase of the activation energy of primary crystallization, accompanied by an increase of the amount of non-crystallized phase quenched after the first crystallization peak and by an increase of the thermal stability of the supercooled liquid with increasing Ag_2Se content, suggest that the mechanism of primary crystallization close to the $Ag_{0.25}As_{0.25}Se_{0.50}$ composition is most probably eutectic nucleation, whereas for compositions close to the amorphous–crystalline boundary the mechanism is most probably diffusion controlled growth. Further electron microscopy and isothermal annealing

experiments would be necessary to determine the details of the crystallization processes.

Acknowledgements

The financial support from the Spanish Interministerial Commission for Science and Technology for N. Zotov is highly appreciated.

References

[1] Z. U. Borisova, Glassy Semiconductors, Plenum Press, New York, 1981, p. 334.
[2] C. Carcaly and D. Houphouet-Boigny, J. Non-Cryst. Solids, 86 (1986) 271.
[3] F. Bellido, P. Villares and R. Jimenez-Garay, in: L.D. Pye, W.C. LaCrouse, H.J. Stevens, Eds., The Physics of Non-Crystalline Solids, Taylor and Francis, London, 1992, p. 77.
[4] F. Bellido, J. Vazquez, P. Villarez and R. Jimenez-Garay, Physica Scripta, 50 (1994) 566.
[5] C.J. Benmore and P.S. Salmon, J. Non-Cryst. Solids, 156 and 158 (1993) 720.
[6] C.J. Benmore and P.S. Salmon, Phys. Rev. Letters, 73 (1994) 264.
[7] V. Mastelaro, S. Banazeth, H. Dexpert, A. Ibanez and R. Ollitrault-Fichet, J. Non-Cryst. Solids, 151 (1992) 1.
[8] N. Zotov, F. Bellido and R. Jimenez-Garay, J. Non-Cryst. Solids, 209 (1997) 149–158.
[9] S.R. Elliot, The Physics of Amorphous Materials, Longman Scientific Technical, New York, 1990.
[10] L. Tichy and H. Ticha, J. Non-Cryst. Solids, 189 (1995) 141.
[11] D. Houphouet-Boigny, R. Ollitrault-Fichet, R. Ehoile and J. Flahaut, Mat. Res. Bull., 22 (1987) 169.
[12] J. Jäckle, Rep. Prog. Phys., 49 (1986) 171.
[13] R. Zallen, The Physics of Amorphous Materials, John Wiley and Sons, New York, 1983, p.3.
[14] M. Lasocka, Mat. Sci. Eng., 23 (1976) 173.
[15] C.T. Moynihan, A.J. Eastel, J. Wilder and J. Tucker, J. Phys. Chem., 78 (1974) 2673.
[16] C. Wagner, J. Vazquez, P. Villares and R. Jimenez-Garay, Mat. Chem. Phys., 38 (1994) 74.
[17] R.A. Ligero, J. Vazquez, P. Villares and R. Jimenez-Garay, J. Mat. Science, 26 (1991) 211.
[18] J. Vazquez, R.A. Ligeo, P. Villares and R. Jimenez-Garay, Thermochim. Acta, 157 (1990) 181.
[19] H. Yinnon and D.R. Uhlman, J. Non-Cryst. Solids, 54 (1983) 253.
[20] R.A. Ligero, J. Vazquez, M. Casas-Ruiz and R. Jimenez-Garay, Thermochim. Acta, 197 (1992) 319.
[21] Y.Q. Gao and W. Wang, J. Non-Cryst. Solids, 81 (1986) 129.
[22] C. Wagner, P. Villares, J. Vazquez and R. Jimenez-Garay, Mat. Letters, 15 (1993) 370.
[23] S.A. Dembovsky, Phys. Chem. Glasses, 10 (1969) 73.
[24] D.J. Sarrach, J.P. Neufville and W.L. Haworth, J. Non-Cryst. Solids, 22 (1976) 245.
[25] K. Tanaka, Solid State Commun., 54 (1985) 807.
[26] A.N. Sreeram, D.R. Swiler and A.K. Varsheya, J. Non-Cryst. Solids, 127 (1991) 287.
[27] J.L. Philips, J. Non-Cryst. Solids, 34 (1979) 153.
[28] J. Philips and M.F. Thorpe, Solid State Commun., 53 (1985) 699.
[29] U.V. Voroshilov, M.U. Golovei and M.V. Potorii, Sov. Crystallogr., 21 (1976) 595.
[30] K. Sakai, T. Koide and T. Matsumoto, Acta Cryst., B34 (1978) 3326.
[31] D. Houphouet-Boigny, R. Eholie, R. Ollitraul-Fichet and J. Flahaut, J. Less Comm. Metals, 98 (1984) 11.
[32] D. Houphouet-Boigny, R. Eholie, R. Ollitraul-Fichet and J. Flahaut, J. Less Comm. Metals, 105 (1985) 13.